Physical conditions, dynamics and model simulations during the ice-free period of the Young Sound/Tyrolerfjord system

Jørgen Bendtsen[1], Karin E. Gustafsson[1], Søren Rysgaard[2] and Torben Vang[3]

[1]National Environmental Research Institute, Department of Marine Ecology, Frederiksborgvej 399, P. O. Box 358, DK-4000 Roskilde, Denmark
[2]Greenland Institute of Natural Resources, Kivioq 2, Box 570, DK-3900, Greenland
[3]Council of Vejle, Damhaven 12, DK-7100 Vejle, Denmark

Cite as: Bendtsen, J., Gustafsson, K. E., Rysgaard, S. & Vang, T., 2007. Physical conditions, dynamics and model simulations during the ice-free period of the Young Sound/Tyrolerfjord system. In: Rysgaard, S. & Glud, R. N. (Eds.), Carbon cycling in Arctic marine ecosystems: Case study Young Sound. Meddr. Grønland, Bioscience 58: 46-59.

Abstract

The Young Sound/Tyrolerfjord system is a 90 km long and 2–7 km wide sill fjord in northeast Greenland, with a mean depth of 100 m. Observations of the bottom topography are presented from different sections of the fjord system, which has a total volume of 40 km^3 and a surface area of 390 km^2. Hydrographic observations from the summer period show the large influence from the freshwater discharge on the mixed layer depth in the fjord, which, during summer, is less than 5 m, with surface salinity increasing from values below 10 in the inner part of Young Sound to about 30 above the sill in the outer part of the fjord. The deep and intermediate water in the fjord is characterized by a temperature of -1.7 °C and a salinity of 33.1, corresponding to $\sigma_t < 26.5$. The maximum tidal amplitude is 0.8 m and 0.4 m during flood and neap tide, respectively, and is dominated by the lunar semi-diurnal M2 tidal constituent. New model simulations show the evolution of the mixed layer during the summer season. A sensitivity study based on this model is presented, showing that the mixed layer thickness will decrease by about 20 % if the runoff is increased by a factor of two, and the implications for the hydrographic conditions in relation to a global warming scenario are discussed.

3.1 Introduction

The Young Sound/Tyrolerfjord system is a c. 90 km long sill fjord in Northeast Greenland, which has been monitored regularly since 1995 from the research station ZERO (Zackenberg Ecological Research Operations). Outside the fjord (the inner part of the East Greenland Current system) water masses are characterized by relatively low salinity. The East Greenland Current is the major coastal-shelf current system in the Nordic Seas, transporting relatively fresh water from the Arctic Ocean together with "recirculating" Atlantic water from the Fram Strait towards the Denmark Strait (i.e. Rudels et al., 2002 ; Chapter 1). Thus, remote changes in the hydrographic conditions in this area will be reflected in the water masses outside Young Sound. For example, due to its role as a major pathway for fresh water from various sources in the Arctic Mediterranean, such as runoff and melted sea ice, a change in the strength and characteristics of the East Greenland Current can be an indicator, or potentially a measure, of large-scale climatic changes in the polar seas. Such changes have been simulated in several coupled ocean-atmosphere models, which

have shown the climate in the polar regions to be sensitive to changes in atmospheric greenhouse gas concentrations (Roeckner et al., 1999; Houghton et al., 2001). Analyses of long time series of sea ice cover in the Arctic region also indicate significant changes in the climatic conditions (Vinnikov et al., 1999). Decreasing sea ice cover in the Arctic Ocean could change the freshwater content of the East Greenland Current. Such changes would also influence hydrographic conditions inside Young Sound, and, therefore, a description of present hydrographic conditions and an understanding of the dynamics in the fjord is a prerequisite for assessing future changes and the possible impact of climate change in the area.

Large transport of sea ice and frequent calving of icebergs make investigation of the East Greenland Current difficult, which is why the existing dataset of the hydrographic conditions in this region is relatively limited. In particular, coastal observations are nonexistent in many areas, and, consequently, the dynamics here are basically unknown. Observations in the Young Sound provide the first time series of hydrographic conditions from a fjord in this region.

A complete description of the exchange to the open sea from the fjord requires more data on the hydrographic conditions outside the sill than are currently available. However, the fjord represents a typical deep sill fjord and, therefore, the dynamics and hydrography in the fjord can be related to the general dynamics of this type of fjord system (Stigebrandt, 2001). In such systems the water exchange to the open sea is a combination of several circulation processes: (1) The tidally driven barotropic exchange caused by sea level variations outside the fjord, (2) the baroclinic exchange caused by density variations of the coastal waters outside the fjord or due to up- or downwelling inside the fjord due to wind forcing, and (3) the baroclinic estuarine circulation driven by freshwater supply and mixing inside the fjord. The relatively shallow sill at the fjord mouth inhibits the exchange of deeper waters, and the water is therefore generally characterized by (1) a surface layer resulting from the local river discharge and sea ice melt kept well mixed by the wind down to a few meters depth, where a primary pycnocline can be observed, (2) an intermediary layer down to about sill depth with a stratification more or less imported from the coastal water outside the fjord, and (3) dense basin water trapped below sill level. The sill acts as an efficient barrier to ventilation of the deepest water mass and a secondary pycnocline usually develops in the fjord at about or below sill level. Between renewals of deep water the density of the basin water decreases slowly due to turbulent diffusion. Internal waves on the secondary pycnocline may provide energy for turbulent diffusion in the deeper layers of the fjord. In the cold season, cooling and ice formation may create dense water at the surface, resulting in convection, increased vertical mixing and formation of a dense winter water mass contributing to the intermediate and deep waters. These general characteristics are in accordance with the observed conditions in the fjord as shown below.

Photo: Søren Rysgaard

Launching CTD moorings in Young Sound during August 2001.

Results from moorings and synoptic transects are presented together with measurements of the bathymetry of the fjord. These provide the input data for a numerical study of the physical conditions during the summer season in the fjord, where the importance of interannual variability of runoff for the formation of the surface mixed layer is quantified through a model sensitivity study. Finally, the implications of increased runoff due to a warmer climate for the surface conditions in the fjord and the exchange between the fjord and the East Greenland Current are discussed.

3.2 Methods

3.2.1 Physical conditions

The bottom topography of the fjord system was surveyed along predefined transects using a dual-frequency echo sounder and a GPS receiver mounted on a rubber dinghy. A total distance of 850 km was covered and about 200,000 data points were collected (Rysgaard et al., 2003). The data was subsequently interpolated on a regular UTM grid using a method based on triangulation.

CTD measurements were made in the fjord during August 2003 and March 2005. Continuous temperature, salinity and water level measurements were taken from August 2003–July 2004 from a SBE 37 instrument (Sea-Bird Electronics, Inc.) placed at a depth of 63 m near the island Sandøen. The water level record was analyzed for amplitudes and phases for the dominant tidal constituents by the method described in Pawlowicz et al. (2002).

3.2.2 Numerical simulations

A three-dimensional primitive equation model based on the COHERENS model (Luyten et al., 1999) was used for quantifying transports and mixing in the fjord system. The model solves the hydrodynamic equations on a vertical sigma coordinate system. This implies a fixed number of vertical grid levels in the entire model domain, with a logarithmic increase of the grid resolution towards the surface. Mixing processes in the surface boundary layer are parameterized by a k-epsilon turbulence closure scheme, so that the mixing intensity is explicitly described as a function of turbulent diffusive momentum and energy transports across the air/sea interface. The model has a free surface, allowing an explicit description of the tides. The model is driven by hourly meteorological fields of wind, temperature, cloudiness, air pressure and relative humidity generated by an operational weatherforecast model (Brandt et al., 2001). The model is forced with the 8 most significant tidal constituents at the open-sea boundaries. River runoff is based on annual measurements of the Zackenberg River discharge during 2003 (Chapter 2). Furthermore, river runoff from the Zackenberg River, Djævlekløften, Lerbugten and the inner part of the fjord (Tyrolerdal) was quantified during 2005 by monitoring the water level (h) in these rivers every 15 min during the summer thaw by use of automatic diver systems. At each of the localities the amount of discharge (Q) was measured on several occasions during summer of 2005 to ensure that the absolute amount of fresh water from the terrestrial to the marine environment could be quantified from Q/h relations for each specific river. These 4 rivers contribute up to 90 % of the total freshwater runoff to the fjord and the ratio of the discharge from each of them relative to the Zackenberg River is: Zackenberg River 100 %, Djævlekløften 100 %, Lerbugten 100 % and the river in Tyrolerdal 310 %. These ratios cause the total runoff to the fjord to be a factor of 6.1 larger than the runoff from the Zackenberg River, corresponding to the ratio of the total drainage area to the drainage area of the Zackenberg River. The fresh water is assumed to enter the fjord in the upper 5 m of the water column at the river mouth. The bathymetry of the model is based on the gridded data set described above, and these data are averaged on a 1×1-km horizontal grid in the model domain. Outside the fjord, the bathymetry is based on the global 2-minute-gridded elevation data ETOPO2 (ETOPO2, 2001) and the landmask is based on the GLOBE data set (Hastings & Dunbarr, 1999). The model has 15 vertical grid levels and it is integrated during the period from 1 March to 1 September 2003. The model is initialised with temperature and salinity fields obtained in the deepest part of Tyrolerfjord in March 2005 (at the station "Dybet"). The open-sea boundary conditions of temperature and salinity are linearly interpolated in time between observed profiles of T and S from March to August. The horizontal diffusion is increased to 500 $m^2\ s^{-1}$ in a diffusive buffer layer 8 km wide along the open-sea boundaries, outside which it is zero. This buffer zone smoothes the temperature and salinity gradients close to the open boundaries but its influence on the conditions inside the fjord is limited. The formulation and assumptions of the open-sea boundary conditions are discussed further below.

3.3 Results & discussion

3.3.1 Bathymetry

The Young Sound/Tyrolerfjord system is a sill fjord located in Northeast Greenland between 22 °W–20 °W and 75.2 °N–74.6 °N. The Tyrolerfjord constitutes the narrow innermost part of the fjord system and Young Sound the wider outer part towards the open sea and

the East Greenland Current system (Fig. 3.1). The fjord system is about 90 km long and 2–7 km wide and covers an area of 390 km^2. The volume of the fjord system is 40 km^3 corresponding to a mean depth of 100 m (Tables 3.1 and 3.2). The sill depth in Young Sound is only 45 m and, therefore, more than 60% of the water volume in the system is located below the sill. The deepest part of the fjord system is located in Tyrolerfjord, with a maximum depth of 360 m. The Young Sound (areas 1, 2 and 3, Fig. 3.1) and outer part of the Tyrolerfjord (area 4) constitute 44 % and 30 % of the total volume, corresponding to a mean depth of 91 m and 183 m, respectively. The inner part of the fjord (areas 5 and 6) has a mean depth of 80 m.

3.3.2 Hydrography and tides

The hydrographic conditions in the fjord system are affected by estuarine circulation during the ice-free period because of the large freshwater input from the melting of snow and ice in the drainage area. The shallow sill reduces the exchange with the open sea, disconnecting the deepest part of the fjord from the East Greenland Current during most of the year. During winter, the fjord is covered with sea ice, which typically starts to melt in May-June when the surface air temperature increases, and complete breakup of the sea ice then takes place during mid-summer (see Chapter 4). The total drainage area to the fjord system is 3109 km^2 and the runoff typically starts in June and ends in August–September. The Zackenberg River drainage area is 512 km^2 and runs into Young Sound. Measurements show a large interannual variability of the discharge into Young Sound with a total runoff during the summer period ranging between 174 and 256 million m^3 for the years 1997–1999 (Chapter 2; Rysgaard et al., 2003).

The hydrographic conditions during August 2003 along a transect from the inner part of the fjord to the East Greenland Current shows the separation between the upper water masses above the sill depth and the deeper part of the fjord (Fig. 3.2). The deepest water mass below 300 m depth in the fjord is characterized by a temperature below -1.7 °C and a relatively high salinity – above 33.15 – corresponding to a density, σ_t, of 26.68. Between the sill depth and 300 m depth the salinity increases gradually from 33.1 to 33.15 and the temperature is about -1.7 °C. The bottom water masses near the sill are modified by water entering from the

Figure 3.1 (a) Relief model of Young Sound. **(b)** Cross-section at the sill in the outer part of Young Sound. **(c)** The Young Sound/Tyrolerfjord system is divided into 7 regions (see Table 3.1). The Tyrolerfjord covers regions 4–6 and Young Sound covers region 1–3. **(d)** Length section of the fjord with marking of regions. Figure adapted from Rysgaard et al. (2003).

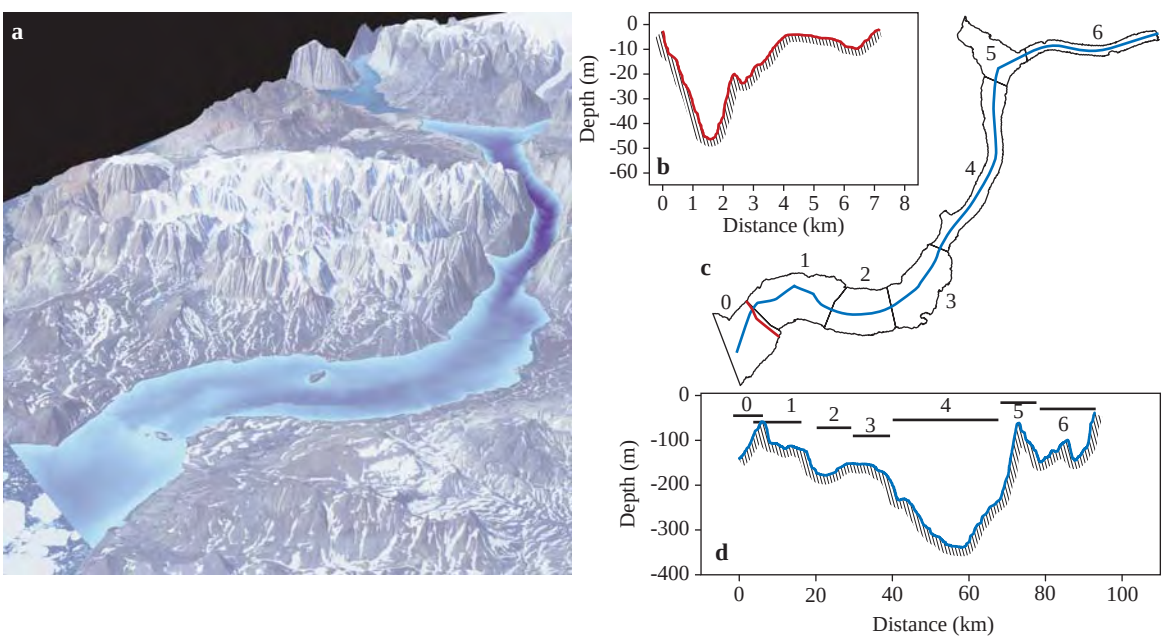

Table 3.1 Hypsometric data from each region of the fjord system. The sea-floor area in the depth intervals is in units of km^2. The table is adapted from Rysgaard et al. (2003).

Depth interval (m)	Region 0	Region 1	Region 2	Region 3	Region 4	Region 5	Region 6	Total (0–6)
0–10	9.827	5.324	1.479	3.521	1.913	3.512	1.473	27.049
10–20	3.958	3.136	1.610	2.578	1.741	2.407	1.424	16.853
20–30	3.427	3.405	1.757	2.465	1.677	2.281	1.469	16.480
30–40	3.288	3.630	1.800	2.509	1.682	2.228	1.528	16.664
40–50	3.828	3.863	1.917	2.558	1.641	2.271	1.585	17.661
50–60	4.668	4.776	2.328	2.308	1.642	2.803	1.680	20.204
60–70	3.868	5.456	2.813	2.452	1.547	2.361	2.063	20.559
70–80	4.078	7.678	3.349	2.770	1.506	1.988	2.098	23.465
80–90	4.139	10.111	5.404	3.036	1.539	1.688	2.052	27.968
90–100	4.214	8.888	3.979	3.425	1.495	1.601	2.320	25.921
100–120	8.263	13.036	6.323	7.574	2.984	2.878	5.083	46.141
120–140	5.274	2.782	7.338	8.724	3.106	3.114	3.761	34.100
140–160	0.929	2.452	7.012	12.600	3.331	3.735	1.299	31.358
160–180	0.000	1.609	6.057	5.026	3.609	2.694	0.172	19.167
180–200	0.000	0.000	0.343	1.706	3.999	2.005	0.010	8.062
200–250	0.000	0.000	0.000	0.305	13.754	4.204	0.000	18.263
250–300	0.000	0.000	0.000	0.000	11.813	0.000	0.000	11.813
300–360	0.000	0.000	0.000	0.000	7.637	0.000	0.000	7.637
Total area	**59.759**	**76.144**	**53.508**	**63.556**	**66.615**	**41.767**	**28.016**	**389.366**

Table 3.2 Volume (km^3) in depth intervals in the Young Sound/Tyrolerfjord system. Table adapted from Rysgaard et al. (2003).

Depth interval (m)	Region 0	Region 1	Region 2	Region 3	Region 4	Region 5	Region 6	Total (0–6)
0–10	0.556	0.734	0.529	0.616	0.657	0.399	0.273	3.764
10–20	0.484	0.694	0.513	0.589	0.639	0.372	0.259	3.550
20–30	0.448	0.662	0.496	0.563	0.622	0.348	0.245	3.385
30–40	0.414	0.627	0.479	0.539	0.605	0.326	0.230	3.219
40–50	0.380	0.590	0.460	0.513	0.589	0.303	0.214	3.048
50–60	0.338	0.548	0.440	0.489	0.572	0.278	0.198	2.863
60–70	0.294	0.496	0.414	0.465	0.556	0.252	0.180	2.657
70–80	0.255	0.433	0.384	0.440	0.541	0.230	0.158	2.440
80–90	0.214	0.346	0.342	0.411	0.526	0.211	0.138	2.187
90–100	0.172	0.245	0.291	0.378	0.511	0.195	0.116	1.909
100–120	0.219	0.266	0.478	0.650	0.977	0.345	0.155	3.089
120–140	0.072	0.104	0.349	0.489	0.916	0.288	0.064	2.281
140–160	0.004	0.061	0.196	0.269	0.851	0.214	0.013	1.608
160–180	0.000	0.010	0.066	0.084	0.783	0.151	0.002	1.095
180–200	0.000	0.000	0.001	0.020	0.707	0.104	0.000	0.832
200–250	0.000	0.000	0.000	0.002	1.341	0.079	0.000	1.422
250–300	0.000	0.000	0.000	0.000	0.679	0.000	0.000	0.679
300–360	0.000	0.000	0.000	0.000	0.169	0.000	0.000	0.169
Total volume	**3.849**	**5.816**	**5.437**	**6.517**	**12.240**	**4.095**	**2.245**	**40.199**

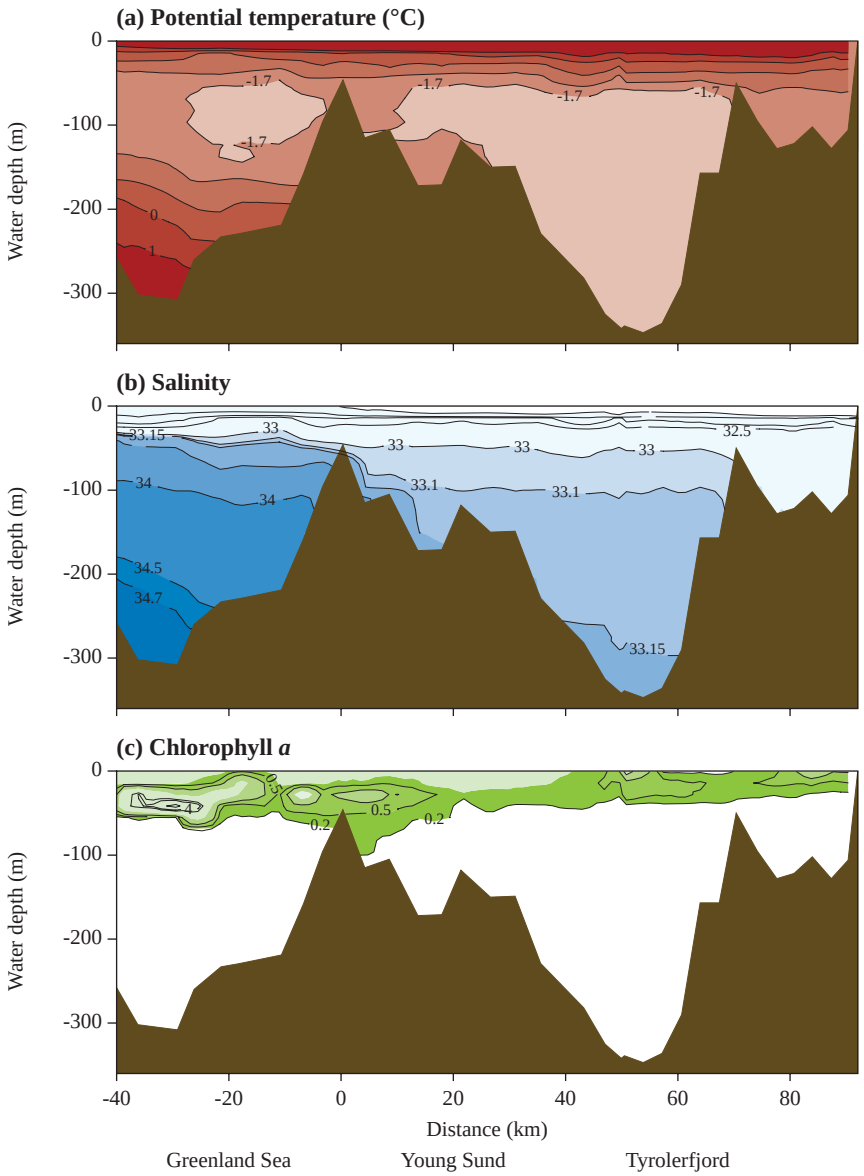

Figure 3.2 (a) Temperature, **(b)** salinity and **(c)** chlorophyll *a* in central Young Sound/Tyrolerfjord and in the inner part of the East Greenland Current system. The distance to the sill (0 km) of Young Sound is shown at the abscissa. Figure adapted from Rysgaard et al. (2005).

East Greenland Current and, therefore, temperatures and salinities are higher here than in the interior of the fjord. The salinity decreases towards the surface to about 30 and the temperature reaches about 2 °C at 5 m depth, corresponding to a σ_t of about 24 (Fig. 3.3). The mixed layer is only about 5 m deep in the fjord and is separated from the underlying water by a strong halocline. In the upper 5 m salinity and temperature change significantly from the inner to the outer part of the fjord, with temperature decreasing from 9 to 2 °C and salinity increasing from about 8 to 30 (Fig. 3.4). Due to the action of the Coriolis force the plume of relatively fresh water is concentrated in the southern part of the fjord, and this causes a slight deepening of the mixed layer of about 1 m in the outer part of Young Sound (Fig. 3.4a, c). The large horizontal variations seen in temperature and salinity distribution in the interior indicate the presence of internal waves in Young Sound between Zackenberg and the sill, with an internal wave amplitude of about 5 m (Fig. 3.4b, d). At present, no time series exist that confirm the frequency of these waves, so it cannot be determined whether they are progressive or not. Progressive components dissipate in the fjord, whereby they contribute to the mixing in the fjord.

The tidal amplitude has a maximum of about 0.8

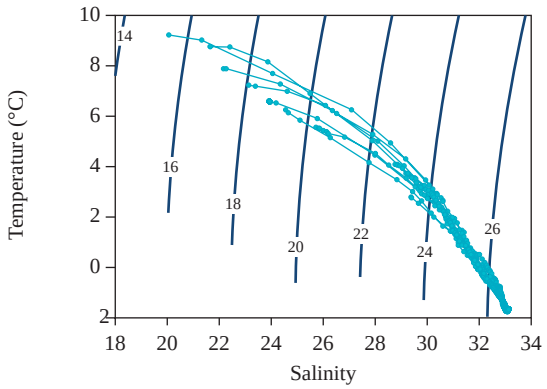

Figure 3.3 T-S plot of CTD profiles taken from a transect from the inner to the outer part of the fjord during August 2004. Contour lines of σ_t are shown.

m during spring flood at the entrance to the fjord and a minimum during neap tide of about 0.3 m (Fig. 3.5). The dominant constituent is the semi-diurnal lunar component M2 with amplitude 0.48 m, and the second and third most important constituents are S2 and K1 with amplitudes 0.18 m and 0.10 m, respectively (Table 3.3). This is in accordance with observations from current-meter moorings in the East Greenland Current system at 75 °N where analysis of currents in the water column showed a similar relative importance of the tidal constituents (Woodgate et al., 1999). Surface currents near Sandøen during August have been observed to reach a maximum value of 1.20 m s^{-1} and have a mean of 0.45 m^{-1} (Rysgaard et al., 2003). The long wave phase speed of the tidal wave gives a time lag of about 48 minutes

Figure 3.4 (a) Salinity and **(b)** temperature (°C) across the sill in the outer part of the fjord. **(c)** Salinity and **(d)** temperature along the centre of Young Sound. The horizontal resolution of measurements are 0.5 km in (**a,b**) and 2 km in (**c,d**), respectively, and 20 cm in the vertical. Figure adapted from Rysgaard et al. (2003).

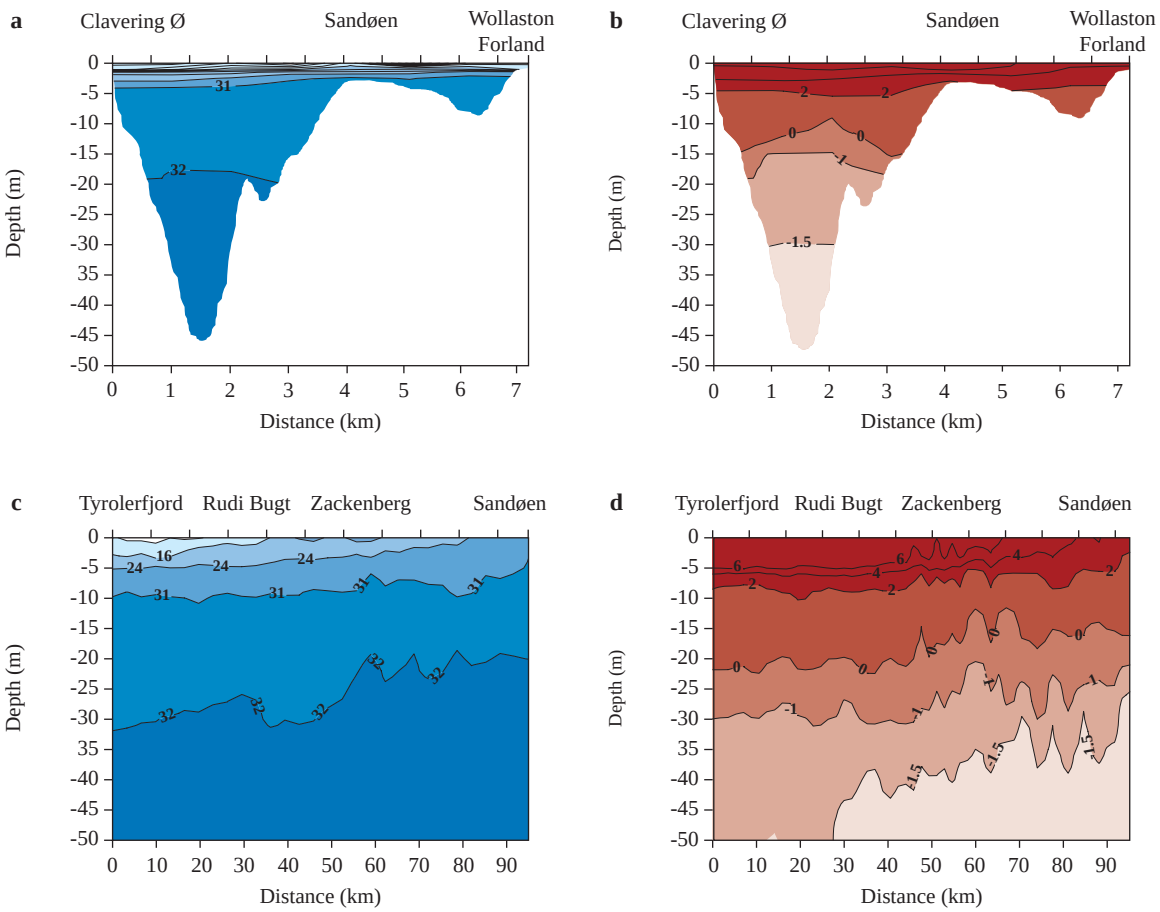

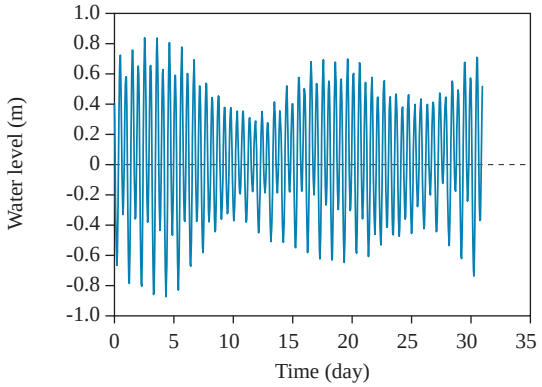

Figure 3.5 Water level measured near the island Sandøen in Young Sound in the period 1–31 July 2004.

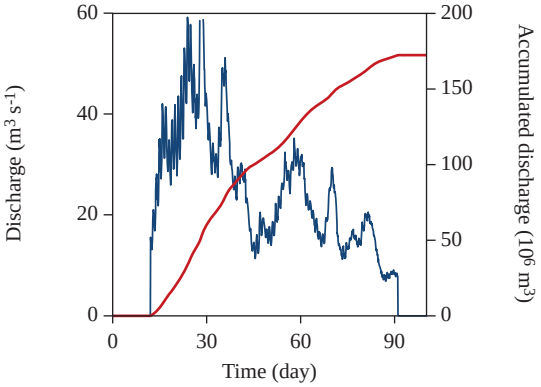

Figure 3.6 Freshwater discharge from the Zackenberg River in 2003 (blue line) and the accumulated discharge (red line). The time axis starts 1 June, and the discharge begins 13 June and ends 21 August.

Table 3.3 Tidal components and amplitudes for the 9 most important tidal constituents, based on data from an SBE-logger during August 2003–August 2004.

Tidal component	Period (hours)	Amplitude
SSA Solar semi-annual	4382.1	0.0386
MF Lunar fortnightly	327.8	0.0232
O1 Principal lunar diurnal	25.82	0.0802
P1 Principal solar diurnal	24.07	0.0319
K1 Luni-solar diurnal	23.93	0.0958
N2 Larger lunar elliptic	12.66	0.0936
M2 Principal lunar	12.42	0.4786
S2 Principal solar	12.00	0.1824
K2 Luni-solar semi-diurnal	11.97	0.0515

between the sill and the inner part of the fjord, and only about 17 minutes at the Zackenberg Station, which is located approximately 30 km from the sill, in accordance with the observed phase lag there.

3.3.3 Simulation of summer conditions

Numerical simulation of the hydrographic conditions during the ice-free summer period described the evolution of the three-dimensional distribution of temperature, salinity and currents together with the two-dimensional field of the water level in the fjord. The existing data set of the hydrographic conditions outside the fjord is very limited, so a detailed description of the time-varying density field in the water column is not yet possible even on a seasonal basis. The boundary conditions outside the fjord are therefore prescribed from a profile of temperature and salinity taken inside the fjord in mid-March and linearly interpolated in time to a profile taken outside the fjord in August. The coarse time resolution of the boundary conditions exclude processes potentially important for the exchange between the fjord and the East Greenland Current system such as short-term changes in the density field due to traveling waves along the Greenland coast or coastal wind surge effects on the water level. The temporal and spatial distribution of sea ice is likewise poorly described through the spring and summer season and, in particular, estimates of sea ice import or export from the fjord are not available, meaning that the influence of these processes on the surface salinity can not be determined. Therefore, the effect of sea ice is disregarded in the analysis below.

Within these limitations the model describes the conditions during the summer season. During this period, the salinity distribution is largely controlled by the freshwater runoff. The runoff is based on the observed river discharge from the Zackenberg River in 2003, which starts on 13 June and ends on 30 August, giving a total accumulated discharge of 172 million m^3 (Fig. 3.6).

In June, the monthly averaged model solution of surface salinity has decreased from the early spring value of about 33 to between 20 and 30 in the inner part of the fjord due to the large river discharge and limited exchange with the rest of Tyrolerfjord,

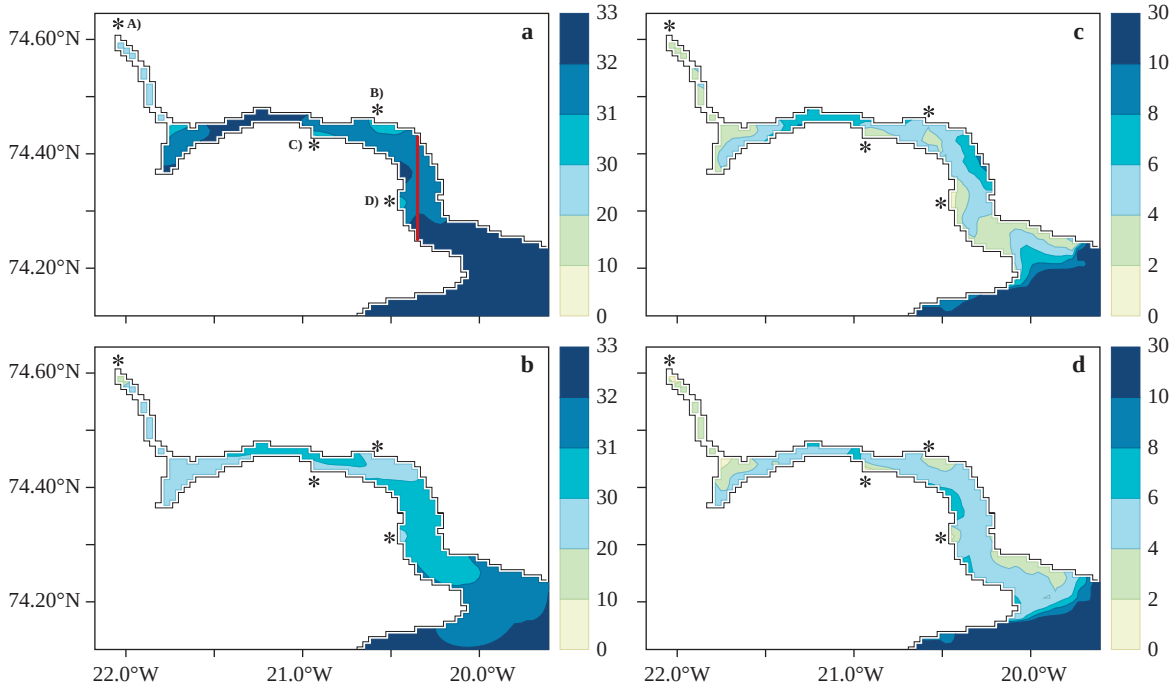

Figure 3.7 Model solutions of monthly averaged surface salinity in June **(a)** and August **(b)** in 2003. The mixed layer depth (m), defined by the depth level with the steepest density gradient in June **(c)** and August **(d)**. The locations of the four rivers are indicated by stars and shown in **(a)** as A) river in Tyrolerdal, (B) Zackenberg, (C) Lerbugten and (D) Djævlekløften. The red line along 20.35 °W in **(a)** shows the transect shown in Figure 3.9. Note that the model solution for June disregards the influence from sea ice.

whereas the salinity distribution in Tyrolerfjord and in Young Sound still exhibits salinities above 31 (Fig. 3.7). In August, the surface salinity has decreased to 30-31 in Young Sound, and decreases gradually towards the inner Tyrolerfjord. The river discharge creates a strong pycnocline in the upper 5-10 m, referred to below as the mixed layer. Already in June the monthly averaged mixed layer depth, defined by the depth having the largest vertical density gradient, is significantly influenced by the freshwater discharge, the mixed layer depth being less than 4 m in the inner Tyrolerfjord and between 4 and 8 m in the central Tyrolerfjord and Young Sound. In August, the mixed layer depth has decreased to 4-6 m in Young Sound and Tyrolerfjord and between 2 and 4 m in the inner part of the fjord. The salinity distribution on a transect across Young Sound shows the deepening of the shallow low-salinity surface layer toward the

Figure 3.8 Model solutions of monthly averaged temperature (°C, red color) and salinity (contour) in a transect across Young Sound at 74.29 °N as a function of depth (m) in July 2003.

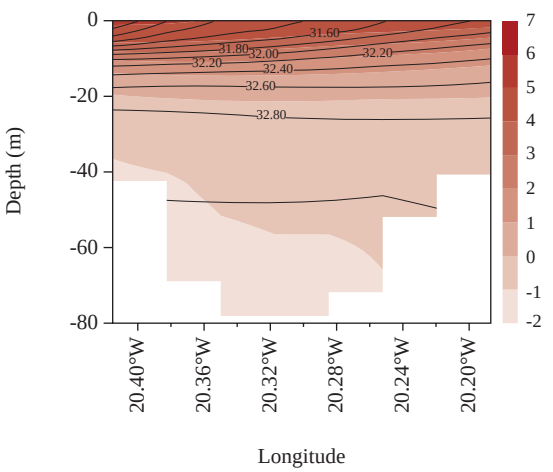

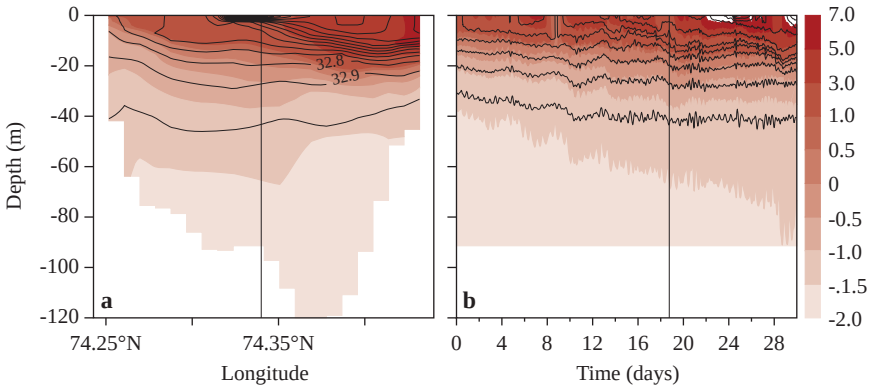

Figure 3.9 (a) Model solutions of temperature (°C, red color) and salinity (contour) along a transect at 20.35 °W on 18 June 2003, covering the central part of Young Sound. **(b)** Time series of the vertical distribution of temperature and salinity (contour) at 74.34 °N and 20.35 °W. The vertical line in **(a)** corresponds to the location used in **(b)**, and the vertical line in **(b)** corresponds to the time for the section shown in **(a)**. Contour intervals are 0.1.

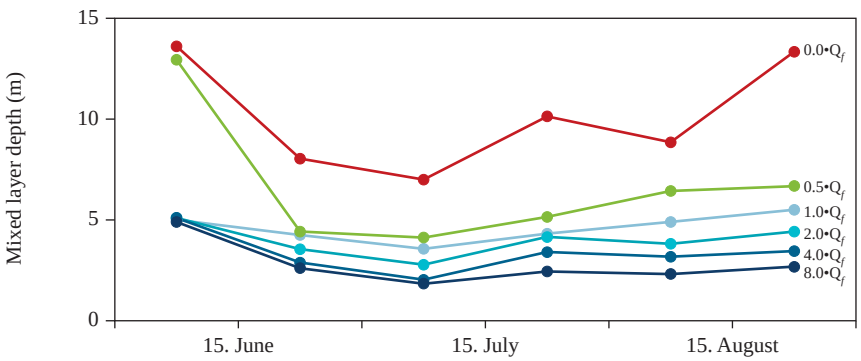

Figure 3.10 Model solutions from the sensitivity study of the relation between the mixed layer depth and the freshwater discharge (Q_f) for 2003 scaled with a constant in each model run. The mixed layer depth is averaged in 14-day intervals from June–August, at the location 20.68 °W; 74.44 °N (see also Table 3.4).

"eastern" coast (Fig. 3.8), i.e. the coast located to the right of the outflowing surface water, in accordance with the observed distributions shown in Fig. 3.4. The depth of the mixed layer is regulated mainly by the salinity distribution, and, therefore, the temperature near the surface has a similar distribution.

Model solutions of a north-to-south transect in Young Sound from 18 June show the newly developed halocline, a mixed layer depth of about 8 m in the northern part of the section and warm water in the mixed layer (Fig. 3.9a). A time series from a location in central Young Sound shows the onset of the halocline in mid-June and the gradual heating of the water column (Fig. 3.9b). The time series also shows propagation of internal waves causing fluctuations on the pycnocline, with small-amplitude oscillations associated with the M2 tidal period of about 1 m, and larger oscillations with amplitude about 5 m and a period of about 4 days, which could be associated with an internal seiche in the fjord.

3.3.4 Sensitivity study in relation to climate change

In a warmer climate, the runoff from land would increase and this would change the circulation and influence the biological production in the fjord. The sensitivity of the fjord to changing runoff was analysed by integrating the model in the period from June to August with different scalings of the total runoff (Fig. 3.10). In the limiting case with no river discharge, the mixed layer thickness is about 9–11 m during the summer season, due to the weak pycnocline in the upper part of the water column (Table 3.4, $\lambda = 0$). At a runoff corresponding to only 50 % of the runoff in 2003 ($\lambda = 0.5$), the halocline is established quite quickly, and the mixed layer is about 0.7–1.6 m

Table 3.4
Monthly averaged mixed layer depth and standard deviation for model solutions with different freshwater discharge Q_f. The mixed layer depth is calculated at the position 20.68 °W, 74.44 °N, corresponding to a locality near the entrance to Tyrolerfjord. The freshwater discharge is scaled with λ in 6 different model runs, such that λ = 1 corresponds to the reference case with a total discharge based on the Zackenberg river discharge observed in 2003.

λ	*0*	*0.5*	*1.0*	*2.0*	*4.0*	*8.0*
June	10.7±5.9	8.5±6.3	4.6±2.8	4.3±2.8	4.0±2.8	3.7±2.8
July	8.7±3.8	4.7±1.9	4.0±1.6	3.5±1.4	2.8±1.2	2.2±0.7
August	11.2±3.1	6.6±2.1	5.2±1.3	4.1±1.1	3.3±1.0	2.5±1.0

deeper in July and August (than in the reference case) (λ = 1.0). In the reference case the mixed layer depth is 4.0 m and 5.2 m in July and August, respectively. At a runoff two times larger than in the reference case (λ = 2.0), the mixed layer becomes about 0.3–1.1 m shallower during the season than in the reference case, and, in an extreme case when runoff is 8 times larger (λ = 8.0), the mixed layer depth decreases to about 2.2–3.7 m during the season. The standard deviation of the monthly averaged mixed layer depth in the reference case and in case of a runoff twice as large, is 1.6 m to 1.4 m in July, and decreases to 1.3 m to 1.0 m in August, respectively.

The sensitivity study shows the importance of the runoff for controlling the depth of the mixed layer. In the case without runoff the mixed layer is controlled solely by wind-induced mixing and buoyancy fluxes at the surface. Even at a moderate runoff of only 50 % of the present level, a freshwater-controlled mixed layer is established quite early by the end of June (Fig. 3.10), and is only slightly deeper than in the reference case. In the other extreme, when runoff is large, the mixed layer depth is controlled by the strength of the surface forcing on the system, i.e. wind and air temperature. Thus, the case with no runoff puts an upper limit on the mixed layer depth of about 11 m in Young Sound during the summer season, and, correspondingly, the case when runoff is 8 times the current level puts a lower limit on the mixed layer depth of about 2 m. The reference case lies between these extremes, and, therefore, a change in runoff can influence the mixed layer depth distribution in the fjord. Doubling of the runoff will decrease the mixed layer by about 1 m or about 20 %. An increase in runoff also reduces the variability of the mixed layer because of the weaker mixing across the stronger vertical pycnocline. In a warmer climate, reduced variability could reduce new production due to further nutrient limitation above the pycnocline during the summer period. However, reduced sea ice cover in the early summer period could increase wind-induced vertical mixing which would have the opposite effect on new production.

In a future, warmer, climate scenario the runoff period might increase significantly, and this would prolong the period in which the surface conditions are controlled by freshwater discharge. However, this

Figure 3.11 (a) Bathymetry and land mask (resolution 2 and 0.5 nm, respectively) along the East Greenland coast off Young Sound (ETOPO2, 2001, Hastings et al., 1999). Hydrographical distributions of salinity and temperature (°C) (contour) along 74 °N, based on World Ocean Atlas 2001 (Conkright et al., 2002) for February **(b)** and August **(c)**.

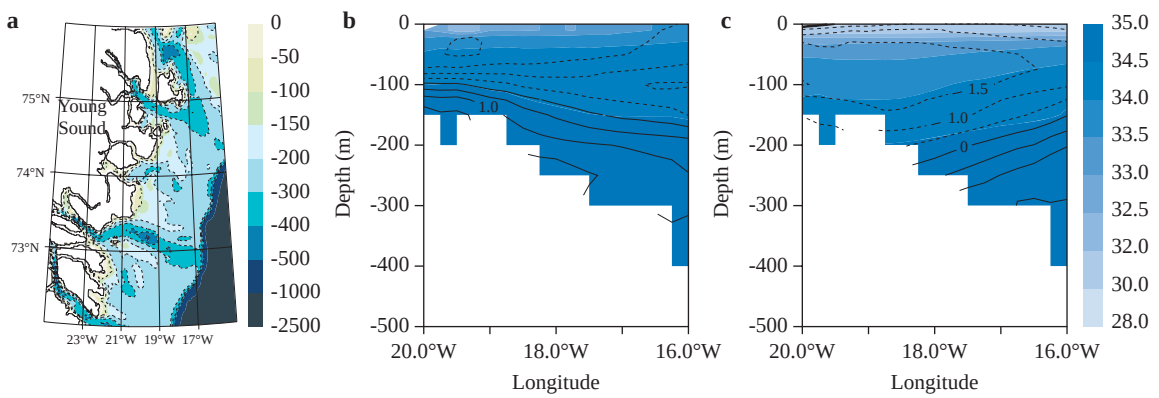

Photo: Søren Rysgaard

Research boat “Aage V. Jensen” in Young Sound at midnight, August 2004.

would not be expected to decrease the mixed layer depth below the solutions shown in Figure 3.10 significantly, as the balance between runoff and atmospheric forcing is established within a few weeks.

3.3.5 Exchanges with the East Greenland Current

During the summer season, the water masses in Young Sound have a relatively low σ_t, between 13 and 26.6 (cf. Fig. 3.3), and transports from the fjord therefore primarily influence the upper water masses of the East Greenland Current system. The East Greenland Current extends across the 100 km wide shelf outside the sill, with typical depth levels of less than 500 m (Fig. 3.11a). The water masses outside the sill in the depth range 50-300 m show large interseasonal changes. During summer, water above 200 m can be characterized as Polar Surface Water (PSW: $\sigma_t < 27.70$, $\leq 0\,°C$) with low temperature and salinity (Rudels et al., 2005; Chapter 1). This water originates from the surface waters in the Arctic Ocean where runoff and meltwater from sea ice cause salinity and temperature to be low. Below 200 m a relatively warm ($\theta > 1\,°C$) and saline ($S > 34.5$) water mass can be identified (Fig. 3.11c, Fig. 3.2). This water mass consists of Arctic Atlantic Water (AAW: $27.70 < \sigma_t < 27.97$, $0 < \theta \leq 2$), which also originates in the Arctic Ocean but may be modified by mixing with warmer and more saline recirculating Atlantic water from the Fram Strait. During winter, the density structure of the East Greenland Current

system changes due to a decrease in low-salinity surface water, and, consequently, the warm and denser AAW moves to depth levels between 100 and 200 m. This water mass will therefore have a larger influence on the characteristics of the deep water entering the fjord from autumn to late winter. Due to the relatively low salinity in the fjord (S < 33.2), there is probably no significant exchange of deep water from the fjord to the East Greenland Current. Even during winter when sea ice formation can increase salinity, the density of the bottom water will remain below the AAW. Density changes outside the sill on shorter time scales, i.e. days to weeks, can have a significant influence on the exchange of water across the sill, but these features can not be resolved from the current observational data set. Current-meter moorings at 74.5–75 °N across the continental shelf and slope show that the core of the East Greenland Current is located above the slope relatively far from the coast with an annual mean southward velocity of 0.16 m s^{-1} in the surface layer. The observed currents are intensified during winter due to the wind-driven gyre transport in the Greenland Sea being stronger during this period of the year (Woodgate et al., 1999).

Apart from the transport associated with the density field, tides (barotropic exchange) and runoff from land contribute significantly to the exchange. The large barotropic exchange associated with the tidal wave corresponds to about 1–2 % of the volume in the fjord twice a day, a relatively high value compared with the runoff from land, which corresponds to about 0.5 % over a 3-month period. However, the estuarine circulation caused by river runoff is amplified by about an order of magnitude due to the relatively small salinity difference between the surface and intermediate layer at the sill, and, therefore, the estuarine circulation becomes a significant part of the exchange. An estimate of the estuarine exchange through Young Sound during a 3-week period in August 2000 shows that transport in intermediate layers results in a net transport of organic carbon into Young Sound of about 15–50 t C day^{-1} (Rysgaard et al., 2003). Calculation of the transport due to the barotropic mode would require a higher spatial resolution of the organic carbon distribution than is available at present, because this transport is controlled to a large extent by the interplay between the horizontal gradients across the sill and the internal vertical mixing in the fjord.

3.4 Acknowledgements

This work was financially supported by DANCEA (the Danish Cooperation for the Environment in the Arctic) under the Danish Ministry of the Environment. This work is a contribution to the Zackenberg Basic and Nuuk Basic programs in Greenland. Aage V Jensens Charity Foundation is thanked for providing financial support for research facilities in Young Sound.

Comments from 3 reviewers as well as linguistic corrections by Anna Haxen improved the manuscript.

3.5 References

Brandt, J., Christensen, J. H., Frohn, L. M., Palmgren, F., Berkowicz, R. & Zlatev, Z. 2001. Operational air pollution forecasts from European to local scale. Atmos. Environ. 35:91-98.

Conkright, M. E., Locarnini, R. A., Garcia, H. E., O'Brien, T. D., Boyer, T. P., Stephens, C. & J. I. Antonov. 2002. World Ocean Atlas 2001: Objective analyses, data statistics, and figures, CD-ROM Documentation, National Oceanographic Data Center, Silver Spring, MD, 17 pp.

ETOPO2, U. S. Department of Commerce, National Oceanic and Atmospheric Administration, National Geophysical Data Center. 2-minute Gridded Global Relief Data, http://www.ngdc.noaa.gov/mgg/fliers/01mgg04.html, 2001.

Hastings, D. A. & Dunbar, P. K. 1999. Global land one-kilometer base elevation (GLOBE) digital elevation model, Documentation, Vol. 1.0, Key to Geophysical records documentation (KGRD) 34. National Oceanic and Atmospheric Administration, National Geophysical Data Center, 325 Broadway, Boulder, Colorado 80303, U.S.A.

Houghton, J. T., Ding, Y., Griggs, D.J., Noguer, M., van der Linden, P. J. & Xiaosu, D. 2001. IPCC Third assessment report: Climate change 2001: The scientific basis, Cambridge University Press, UK.

Luyten, P. J., Jones, J. E., Proctor, R., Tabor, A., Tett, P. & Wild-Allen, K. 1999. COHERENS – A coupled hydrodynamical-ecological model for regional and shelf seas: user documentation. MUMM report, Management Unit of the Mathematical Models of the North Sea, Belgium, 911 pp.

Pawlowicz, R., Beardsley, B. & Lentz, S. 2002. Classical tidal harmonic analysis including error estimates in MATLAB using T_TIDE. Comput. Geosci. 28: 929 – 937.

Roeckner, E., Bengtsson, L. & Feichter, J. 1999. Transient climate change simulations with a coupled atmosphere-ocean GCM including the tropospheric sulfur cycle, J. Clim. 12: 3004-3032.

Rudels, B., Fahrbach, E., Meincke, J., Budéus, G. & Eriksson, P. 2002. The East Greenland Current and its contribution to the Denmark Strait overflow. ICES J. Mar. Sci. 59: 1133-1154.

Rudels, B., Björk, G., Nilsson, J., Windsor, P., Lake, I. & Nohr, C. 2005. The interaction between waters from the Arctic Ocean and the Nordic Seas north of Fram Strait and along the East Greenland Current: results from the Arctic Ocean-02 Oden expedition. J. Mar. Sys. 55: 1–30.

Rysgaard, S., Vang, T., Stjernholm, M., Rasmussen, B., Windelin, A. & Kiilsholm, S. 2003. Physical conditions, carbon transport and climate change impacts in a NE Greenland fjord. Arct. Antarct. Alp. Res. 35: 301–312.

Rysgaard, S., Frandsen, E., Sejr, M., Dalsgaard, T., Blicher, M. E. & Christensen, P. B. 2005. Zackenberg Basic: The marine monitoring programme. In: Rasch, M. & Caning, K. (eds.). Zackenberg ecological research operations 10th annual report, 2004 – Copenhagen, Danish Polar Center, Ministry of Science, Technology and Innovation. 85 pp.

Stigebrandt, A. 2001. Fjord circulation. In: Steele, J., S. Thorpe and K. Turekian (eds.). Encyklopedia of ocean sciences: 897–902. Academic Press Inc., U.S.

Vinnikov, K. Y, Robock, A., Stouffer, R. J., Walsh, J. E., Parkinson, C. L., Cavalieri, D. J., Mitchell, J. F. B., Garret, D. & Zakharov, V. F. 1999. Global warming and northern hemisphere sea ice extent. Science. 286:1934–1937.

Woodgate, R. A., Fahrbach, E. & Rohardt, G. 1999. Structure and transports of the East Greenland Current at 75°N from moored current meters. J. Geophys. Res. 104:18059–18072.